Journal of Structural Biology 196 (2016) 164–172

Contents lists available at ScienceDirect

Journal of Structural Biology

journal homepage: www.elsevier.com/locate/yjsbi

Crystallographic orientation and concentric layers in spicules of calcareous sponges

André Linhares Rossi [a,*], Bárbara Ribeiro [b], Moara Lemos [a], Jacques Werckmann [c], Radovan Borojevic [d], Jane Fromont [e], Michelle Klautau [b], Marcos Farina [c]

[a] Centro Brasileiro de Pesquisas Físicas, Xavier Sigaud, 150, 22290-180 Rio de Janeiro, Brazil
[b] Universidade Federal do Rio de Janeiro, Centro de Ciências da Saúde, Instituto de Biologia, Laboratório de Biologia de Porifera, 21941-590 Rio de Janeiro, Brazil
[c] Universidade Federal do Rio de Janeiro, Centro de Ciências da Saúde, Instituto de Ciências Biomédicas, Laboratório de Biomineralização, 21941-590 Rio de Janeiro, Brazil
[d] Centro de Medicina Regenerativa, Faculdade de Medicina de Petrópolis, Av Barão do Rio Branco, 25680-120 Petrópolis, RJ, Brazil
[e] Western Australian Museum, Department of Aquatic Zoology, Locked Bag 49, Welshpool DC, WA 6986, Australia

ARTICLE INFO

Article history:
Received 15 January 2016
Received in revised form 4 April 2016
Accepted 14 April 2016
Available online 19 April 2016

Keywords:
Biomineralization
Spicule crystallography
Porifera
Calcarea
Calcaronea
Calcinea

ABSTRACT

In this work, the crystallography of calcareous sponges (Porifera) spicules and the organization pattern of the concentric layers present in their inner structure were investigated in 10 species of the subclass Calcaronea and three species of the subclass Calcinea. Polished spicules had specific concentric patterns that varied depending on the plane in which the spicules were sectioned. A 3D model of the concentric layers was created to interpret these patterns and the biomineralization process of the triactine spicules. The morphology of the spicules was compared with the crystallographic orientation of the calcite crystals by analyzing the Kikuchi diffraction patterns using a scanning electron microscope. Triactine spicules from the subclass Calcinea had actines (rays) elongated in the ⟨2$\bar{1}$0⟩ direction, which is perpendicular to the *c*-axis. The scale spicules of the hypercalcified species *Murrayona phanolepis* presented the *c*-axis perpendicular to the plane of the scale, which is in accordance with the crystallography of all other Calcinea. The triactine spicules of the calcaronean species had approximately the same crystallographic orientation with the unpaired actine elongated in the ~[211] direction. Only one Calcaronea species, whose triactine was regular, had a different orientation. Three different crystallographic orientations were found in diactines. Spicules with different morphologies, dimensions and positions in the sponge body had similar crystallographic directions suggesting that the crystallographic orientation of spicules in calcareous sponges is conserved through evolution.

1. Introduction

Sponges (Phylum Porifera) are the oldest extant metazoans. They are simple multicellular animals that do not form true tissues or organs, have a sedentary lifestyle, are filter feeders (with only a few exceptions), and are found mainly in marine environments (Hooper and Van Soest, 2002). The phylum has four extant classes: Demospongiae, Hosmoscleromorpha, Hexactinellida and Calcarea.

Calcarea is the only class of sponges whose skeleton is composed exclusively of calcium carbonate (Mg-calcite) spicules, which behave as a single crystal when observed under polarized light, X-ray diffraction and electron diffraction (Aizenberg et al., 1995; Gilis et al., 2011; Rossi et al., 2014; Sethmann et al., 2006; Sollas and Society, 1885). The calcareous spicules of the extant species are less diverse than the siliceous spicules. There are three basic calcareous spicule: diactines (spicules with two tips), triactines (with three tips), and tetractines (with four tips). This low morphological diversity may be related to the more rigid position of atoms in a calcium carbonate crystal when compared to amorphous materials, such as silica (Uriz, 2006).

Spicules form the sponge skeleton can be random when spicules are found without any order in the sponge body or organized when spicules occupy specific positions. Because both the shape and position of the spicules in the skeleton are considered to be genetically determined, they have been used traditionally as important taxonomic characters (Manuel et al., 2002).

* Corresponding author.
E-mail address: alinhares@cbpf.br (A.L. Rossi).

http://dx.doi.org/10.1016/j.jsb.2016.04.009
1047-8477/

Formation of calcareous spicules and its controls are not fully understood. These spicules are formed extracellularly by cells called sclerocytes. It seems that to form a diactine two sclerocytes are required. For a triactine three sclerocytes are required, and for a tetractine, four are needed (Sethmann and Wörheide, 2008). First, sclerocytes approach each other and form an extracellular space between the cells where they secrete a macromolecular matrix that will guide the deposition of calcium carbonate. The central nucleus of the spicule is, thus, formed, and then, each sclerocyte divides. One sclerocyte (the founder cell) becomes responsible for the length of the actine whereas the other sclerocyte (the thickener cell) will thicken the actine (Ledger and Jones, 1977; Minchin, 1908; Uriz, 2006).

Different from siliceous sponges that synthesize the protein silicatein associated with the spicules, there is no axial filament in calcareous sponge spicules, but the presence of an organic sheath covering the calcareous spicules has previously been reported (Jones, 1955; Kopp et al., 2011). Additionally, the presence of organic molecules within the spicules lead to the final spicule form, which is different from an equivalent inorganic crystal (Aizenberg et al., 1995, 1996). Concentric layers and amorphous calcium carbonate have already been observed in calcareous spicules (Aizenberg et al., 2003; Jones and James, 1972; Kopp et al., 2011).

The class Calcarea is subdivided into two subclasses: Calcinea and Calcaronea. Several characteristics support this deep division. One of these characteristics is the shape of the spicules. In Calcinea, triactine and tetractine spicules are always regular, which means that they have identical angles (120°) between their basal actines that are in the same plane. In the subclass Calcaronea, triactines and tetractines are irregular, *i.e.*, they have a larger angle (>120°) between their paired actines and a have bilateral symmetry (the plane of symmetry contains the unpaired actine). A fourth actine, which is referred to as an apical actine, is found in the tetractines of both subclasses. This actine is not in the same plane of the basal actines but protrudes perpendicularly from the centre of the spicule.

In the present study, we investigated the concentric layers observed as concentric lines in polished sections of calcareous spicules, and the relationship between spicule morphology and the crystallographic orientation of the calcite biocrystal. We analysed diactines and triactines from a variety of calcareous sponge species and compared spicules from Calcinea and Calcaronea. In addition, we discuss the process of biomineralization and spiculogenesis in calcareous sponges.

2. Materials and methods

2.1. Sample preparation

In the present work, 13 species of calcareous sponges were investigated. Table 1 lists the species, classification, voucher numbers and collection sites.

An 80% sodium hypochlorite solution in distilled water was used to isolate the calcium carbonate spicules from the cellular/organic components of the sponges. Three cycles were performed using the sodium hypochlorite solution followed by three cycles using distilled water, and finally, a substitution of the water solution by 100% ethanol. The spicules were air dried and embedded in epoxy resin. The resins containing the spicules were glued in an iron cylinder and further polished using 6, 3, 1 and 0.25 μm diamond paste. The final polishing was performed using a colloidal silicon solution in a vibratory polishing machine (Buehler, Inc.). The spicules surface and the improvement of the polishing process were monitored using a reflected light microscope. The samples were cleaned using distilled water, air dried, and coated with a thin carbon layer (Desk V, Denton).

Table 1
List of species investigated, with their classification, voucher numbers and collection sites.

	Voucher number	Collection site
Subclass Calcinea		
Murrayona phanolepis Kirkpatrick, 1910	M227-GR-TP3*	Marquesas Islands, French Polynesia
Pericharax carteri Poléjaeff, 1883	UFRJPOR 7354	Heron Island, Queensland, Australia
Pericharax sp. nov.	UFRJPOR 7129	Geographe Bay, Western Australia
Subclass Calcaronea		
Grantiopsis cylindrica Dendy, 1892	UFRJPOR 7494	Rottnest Island, Western Australia
Grantiopsis sp. nov.	UFRJPOR 7488	Rottnest Island, Western Australia
Heteropia sp. nov.	UFRJPOR 6151	Forno Beach, Arraial do Cabo, Rio de Janeiro, Brazil
Leucandra cirrhosa (Urban, 1908)	UFRJPOR 4986	Thalassa, Mediterranean
Leucandra serrata Azevedo & Klautau, 2007	UFPEPOR 595	Potiguar Basin, Brazil
Paraleucilla magna Klautau et al., 2004	MNRJ 5147*	Rio de Janeiro, Brazil
Sycettusa hastifera (Row, 1909)	UFRJPOR 5610*	Rio de Janeiro, Brazil
Sycon sp.	UFRJPOR 8379	Twin Peak, Recherche Archipelago, Western Australia
Teichonopsis labyrinthica (Carter, 1878)	UFRJPOR 7107	Leander Pt, Dongara, Western Australia
Ute sp.	UFRJPOR 5010	Thalassa, Mediterranean

* Voucher number from a different specimen from the same species collected in the same site.

2.2. Structural and crystallographic analysis

The polished spicule samples embedded in epoxy resin were analysed in a JEOL JSM-7100F field emission scanning electron microscope (FEG-SEM) equipped with an electron backscattered diffraction (EBSD) detector (Oxford, Inc.). Analyses were conducted using an accelerating voltage of 15 or 20 kV. The Kikuchi patterns were automatically indexed (Aztec software) considering the calcite crystal in the trigonal system (a = b = 0.49 nm and c = 1.70 nm; space group: R-3c). Crystallographic data were exported to HKL Channel 5 software (Oxford, Inc.) from where the Euler angles and Miller indices were obtained. Stereographic projections were constructed using the JEMS software (electron microscopy software java version) to determine the relative crystallographic directions. The results are presented as Miller indices. A model of the triactine spicule in 3D showing the concentric layers was created using the SolidWorks software (Dassault Systèmes S.A.).

2.3. Concentric lines

For the current analysis, triactines from two calcinean (*Murrayona phanolepis*, *Pericharax carteri*) and two calcaronean (*Leucandra cirrhosa*, *Leucandra serrata*) species were investigated. From *M. phanolepis*, we selected to analyse the diapason-like (tuning-fork) spicules. The diapason-like spicules have parallel-paired actines, which means that they are bent to each other and become aligned with the unpaired actine (Boury-Esnault and Rützler, 1997).

From *P. carteri*, we selected large choanosomal regular (equiangular and equiradiate) triactines. From *L. cirrhosa* and *L. serrata*, we

selected choanosomal giant triactines, which are almost regular (equiangular and equiradiate), although these spicules are rare in calcaroneans.

2.4. Morphology and crystallographic orientation

The relationship between the morphology of the spicules and the crystallographic orientations was obtained for three species of the subclass Calcinea and 10 species of the subclass Calcaronea (Table 2). The spicules analysed were triactines and diactines.

The large cortical and regular (equiangular and equiradiate) triactines were analysed from *Pericharax* sp. nov. and *P. carteri*, while the scales and the diapason-like (tuning-fork) spicules were analysed from *M. phanolepis*.

The analysed diactines were from *Grantiopsis cylindrica*, *Grantiopsis* sp. nov., *Heteropia* sp. nov., *L. cirrhosa*, *Sycettusa hastifera*, *Sycon* sp., *Teichonopsis labyrinthica*, and *Ute* sp. The diactines from *Heteropia* sp. nov. and *Ute* sp. are tangentially orientated to the cortex, whereas all others are obliquely or perpendicularly oriented. *Heteropia* sp. nov., *S. hastifera*, and *Ute* sp. have larger diactines and only *Heteropia* sp. nov., *L. cirrhosa* and *Ute* sp. have fusiform diactines. All the other spicules have arrow-shaped diactines or one tip different from the other.

Table 2
Elongation direction of spicules from the subclass Calcaronea and Calcinea. Each species may contain different spicule types (shape, size and position in the sponge). The crystallography data were obtained from some but not all the spicule types from each species. In some cases the spicule could not be related with a specific position in the sponge body.

Spicule elongation directions	
Subclass Calcinea	
M. phanolepis	- Scale spicule (tangential to the surface): *c*-axis perpendicular to the spicules plane - Diapason with actines elongated in the ⟨2 1 0⟩
P. carteri	- Regular triactines (tangential to the cortex) with the actines in the ⟨2 1 0⟩
Pericharax sp. nov.	- Regular triactines (tangential to the cortex) with the actines in the ⟨2 1 0⟩
Subclass Calcaronea	
G. cylindrica	- Sagittal triactines (tangential to the cortex) with the unpaired actine in the ∼[2 1 1] - Diactines[a] elongated in the ∼[2 1 0]
Grantiopsis sp. nov.	- Sagittal triactines (tangential to the cortex) with the unpaired actine in the ∼[2 1 1]. - Diactines[a] elongated in the ∼[2 1 0] and [0 1 1].
Heteropia sp. nov.	- Triactines and pseudosagittal triactines with the unpaired actine in the ∼[2 1 1] - Giant diactines (tangential to the cortex) elongated in the ∼[2 1 0]
L. cirrhosa	- Triactines (tangential to the cortex) with the unpaired actine in the ∼[2 1 1] - Giant triactines (regular and choanosomal) with the actines in the ⟨2 1 0⟩ - Giant diactines (perpendicular to the cortex) elongated in the ∼[2 1 0]
L. serrata	- Giant triactines with the unpaired actine in the ∼[2 1 1]
P. magna	- Sagittal triactines with the unpaired actine in the ∼[2 1 1]
S. hastifera	- Triactines with the unpaired actine in the ∼[2 1 1] - Arrow-shaped diactines (perpendicular to the surface) elongated in the ∼[2 1 0]
Sycon sp.	- Sagittal triactines with the unpaired actine in the ∼[2 1 1] - Diactines (perpendicular to the surface) elongated in the [0 0 1]
T. labyrinthica	- Triactines with the unpaired actine in the ∼[2 1 1] - Lance-shaped diactines elongated in the [0 0 1]
Ute sp.	- Triactines with the unpaired actine in the ∼[2 1 1] - Giant triactines (tangential to the cortex) elongated in the ∼[2 1 1]

[a] *Grantiopsis* sp. nov. and *G. cylindrica* present diactines, chiactines and nails. In the polished sections, these spicule types could not be differentiated.

3. Results

3.1. Concentric lines

The ultrastructure of polished spicules embedded in epoxy resin was analysed by FEG-SEM. Concentric lines with different patterns were observed in the bulk of the spicules in all samples even in the unusual scale spicule from the hypercalcified species *M. phanolepis*. Fig. 1A and B show triactine spicules from *L. serrata* (subclass Calcaronea). These triactines have a similar morphology, and their actines were aligned approximately with the surface of the resin after polishing but at slightly different depths. In Fig. 1A, the more internal concentric patterns were centred in each actine (Fig. 1A, stars). Intermediate concentric lines were observed surrounding two actines (arrow), and the more external lines surrounded the three actines (arrowhead).

Fig. 1B shows a different aspect of the concentric lines. In this case, the origin of the concentric lines was visibly in the centre of the whole spicule and not in each actine as observed in the previous image. Different line patterns were observed likely due to the difference in the depth in which the spicules were polished and not because the spicules were structurally different.

A particular line pattern was systematically observed in the spicule of *P. carteri* (subclass Calcinea). A faceted structure was observed in the centre of the spicule (Fig. 2A, arrowheads and insert). As in the previous case, concentric lines were elongated along the axis of each actine (arrow). The species *L. cirrhosa* (subclass Calcaronea) had only one concentric line near the periphery of the actine in the polished section (Fig. 2B, arrow), which likely represents a different cell positioning and/or a different growth velocity during biomineralization. Fig. 2C shows concentric lines in the diapason-like spicule from the hypercalcified species *M. phanolepis* (subclass Calcinea).

3.2. Morphology and crystallographic orientation

3.2.1. Triactines

The crystallographic orientations of the polished spicules sections were obtained by EBSD. Dispersion of less than 1° was found for adjacent regions spaced by ∼3 μm in the same spicule (Fig. 3). The misorientation profiles shown in Fig. 3 were extracted in a line parallel and transverse to the unpaired actine.

The triactine spicules from *Pericharax* sp. nov. and *P. carteri* (subclass Calcinea) had actines elongated in the ⟨2 1 0⟩ direction (Fig. 4A). The plane containing the actines was perpendicular to [0 0 1] (*c*-axis) (Fig. 4B). The scale spicules from the hypercalcified species *M. phanolepis* (subclass Calcinea) were normal to the [0 0 1] direction (Fig. 4C and D). The diapason-like spicule from *M. phanolepis* had actines elongated in the [2 1 0] direction, and the plane of the spicule was approximately perpendicular to the [0 0 1] direction (Fig. 4E and F).

All triactine spicules from the calcaronean species analysed in this work, with only one exception (the regular triactine from *L. cirrhosa*), had the same crystallographic orientation. The unpaired actine was elongated between the [6 3 2] and the [2 1 1] directions (Fig. 5A, B and C). The [0 1 0] direction was positioned in the plane of the actines and was perpendicular to the unpaired actine (Fig. 5C). The *c-axis* was positioned 27–37° from the unpaired actine in a plane that symmetrically divides the paired actines. The paired actines were elongated in symmetrically related directions.

Calcaronean triactine spicules with different morphologies, for instance, the triactines from *L. cirrhosa* (Fig. 5D and E) and the pseudosagittal triactine from *Heteropia* sp. (Fig. 5F and G), had a similar crystallographic orientation: the unpaired actine elongated

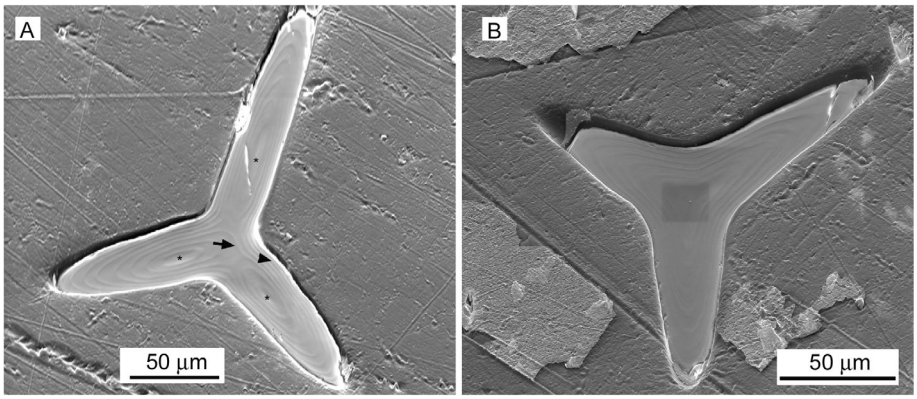

Fig. 1. Polished triactine from *Leucandra serrata* (subclass Calcaronea) observed using SEM showing concentric lines representing concentric layers in different depths of the spicule. (A) In this image, more internal layers are observed to be centred in each actine (stars). Intermediate concentric layers (arrow) surround two actines, and additional external layers surround the three actines (arrowhead). (B) This image shows the origin of the concentric layers in the centre of the whole spicule. The darker rectangle in the centre of the spicule is a carbon layer deposited by the electron beam during scanning.

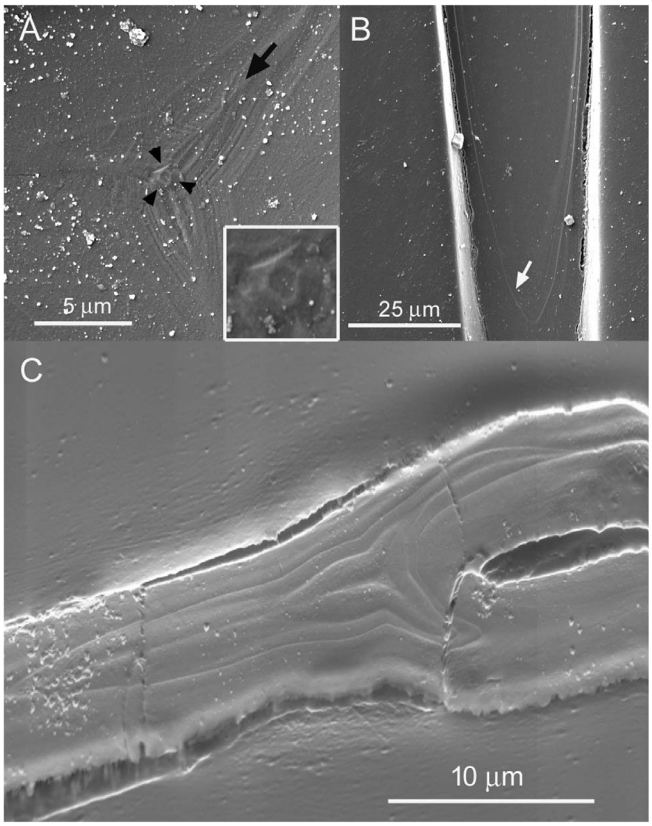

Fig. 2. Concentric layers in polished spicules from the subclass Calcinea and Calcaronea imaged by SEM. (A) Faceted structure observed in the centre of the spicule in the species *P. carteri* (arrowheads and insert). (B) Only one concentric layer near the periphery of the actine was observed in *L. cirrhosa* (arrow). (C) Concentric layers in the diapason spicule from the hypercalcified species *M. phanolepis*.

in the ~[2 1 1] direction and the spicule plane in the same zone axis. Only one Calcaronean species had a triactine spicule with a different crystallographic orientation. The species *L. cirrhosa* has regular and irregular triactine spicules. In the regular spicule, actines were elongated in the ⟨2 1 0⟩ direction, which is similar to the crystallographic orientation found in Calcinea (Fig. 6, left side). The crystallographic orientation of the irregular spicule was similar to that of the other Calcaronean species (Fig. 6, right side).

3.2.2. Diactines

The crystallographic orientation of the diactine spicules was investigated as well. Three orientations were revealed within the species (Fig. 7). Type I orientation (Fig. 7A) had diactines elongated in the ~[2 1 0] direction (*S. hastifera*, *Ute* sp., *Grantiopsis* sp. nov., *L. cirrhosa*, *Heteropia* sp. nov., and *G. cylindrica*). Type II orientation (Fig. 7B) had diactines elongated in the [0 0 1] direction (*Sycon* sp. and *T. labyrinthica*). Type III orientation (Fig. 7C) had diactines elongated in the [0 1 1] direction (*Grantiopsis* sp. nov.). The species *Grantiopsis* sp. nov. had diactines with two orientation types. The crystallographic orientations of diactine and triactine spicules are summarized in Table 2.

4. Discussion

4.1. Concentric layers

The existence of concentric layers in polished spicules of calcareous sponges observed by SEM has been reported previously (Jones and James, 1972; Kopp et al., 2011). This organization pattern has been described as "successive concentric layers", "stratification" and a "concentric lamination pattern" (Sethmann and Wörheide, 2008). Jones and James (1972) and Kopp et al. (2011) described these structures as successive ridges and furrows that form primary (250 nm) and secondary (535 nm) layers, suggesting that less intense concentric layers may exist between the major layers. In the present work distances between adjacent layers were approximately 500 nm (primary layers) or 150 nm (secondary layers). In the case of the giant triactine spicule from *L. serrata*, larger layers spaced by 2 µm were observed. The thicknesses of these layers are in agreement with those reported by Kopp et al. (2011) in the species *Leuconia johnstoni* although in that work polished sections were etched with 0.1% formic acid.

The appearance of different patterns of concentric layers in the same samples may be related to the etching agent (alkaline or acidic etching), its concentration or time of application (Jones and James, 1972). The interpretation of the 3D layers in the spicules is not straightforward because the images obtained after polishing are from sections of a complex 3D volume. According to Jones and James (1972) and Kopp et al. (2011) the concentric layers of each actine would form an ellipsoidal geometry in 3D.

In the species *Leuconia johnstoni*, nanoSIMS and scanning X-ray microscopy were used to show that the central region of the spicule was rich in sulphur, and the shell/envelope region had a greater proportion of magnesium. However, no variation in

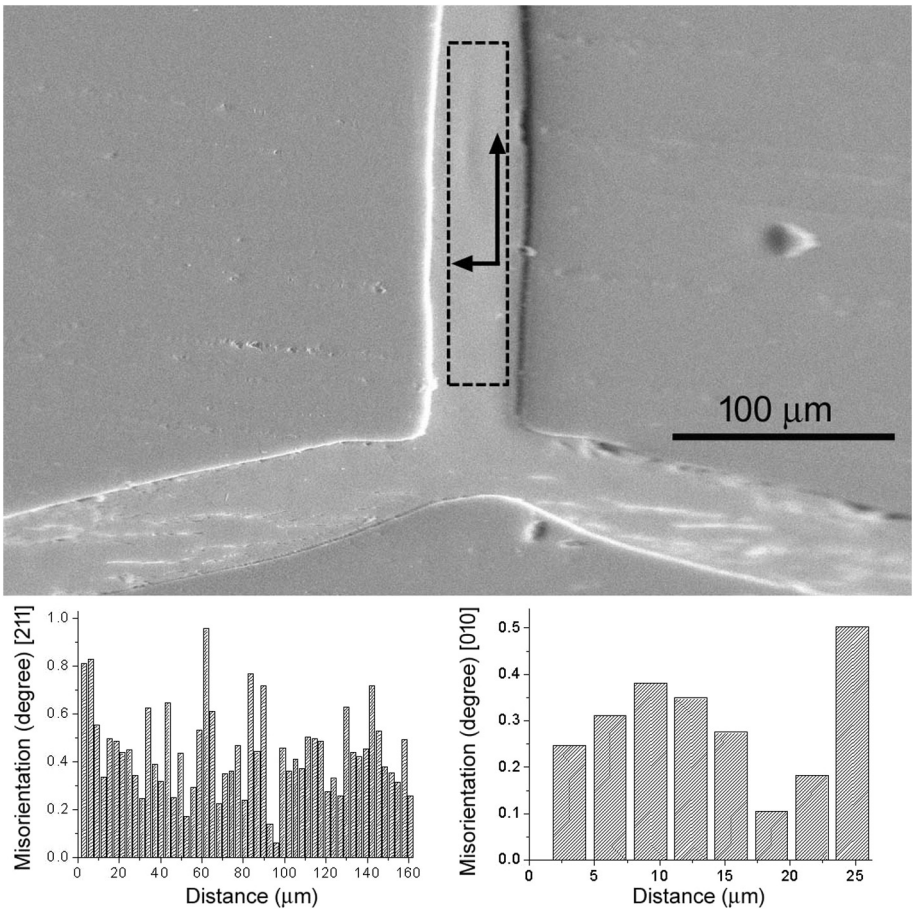

Fig. 3. Crystal misorientation obtained by EBSD analyses in the spicule of *G. cylindrica*. The dashed rectangle in the unpaired actine of the spicule shows the region from where the diffraction data were collected (53 × 9 pixels with each pixel corresponding to one diffraction pattern). The misorientation profiles (lower portion of the figure) were extracted in a line parallel (∼[2 1 1] direction, large arrow) and transverse ([0 1 0] direction, small arrow) to the unpaired actine. Dispersion of less than 1° was found in adjacent regions ∼3 µm apart in the same spicule.

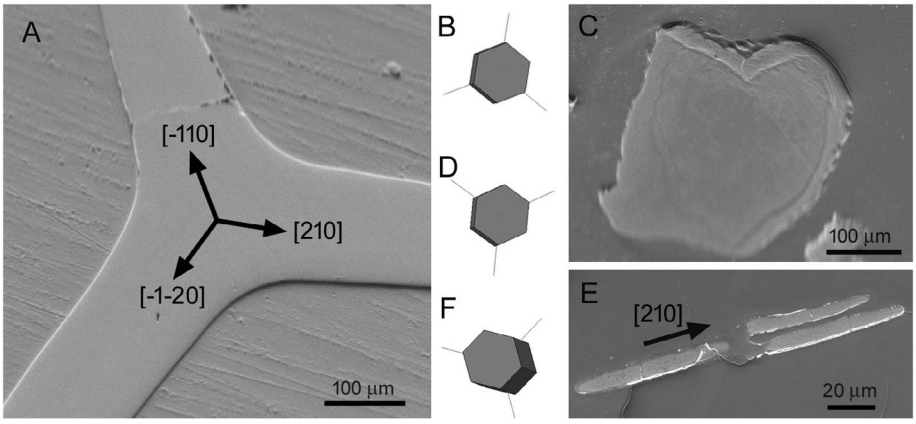

Fig. 4. Crystallographic analyses in the subclass Calcinea. (A) SEM of a triactine spicule from *Pericharax* sp. nov. The arrows show the crystallographic directions of the actines. Each actine was elongated in the ⟨2 1 0⟩ symmetrically related directions (perpendicular to the {1 0 0} plane). (B) Model representing the calcite crystal in 3D. The axes correspond to the ⟨1 0 0⟩ direction. (C) SEM of a scale spicule from *M. phanolepis*. (D) 3D crystal model from (C) indicating that the *c*-axis was perpendicular to the scale. (E) SEM of a diapason spicule from *M. phanolepis*. The arrow shows that the actines were elongated in the [2 1 0] direction. (F) 3D crystal model from (E) indicating that the *c*-axis was approximately perpendicular to the diapason plane.

composition was observed between concentric layers (Kopp et al., 2011). In the present work, as well as in previous works, crystallographic misorientations/interruptions (Rossi et al., 2014) or clear periodic organic layers (Gilis et al., 2011; Kopp et al., 2011; Sethmann et al., 2006) between the adjacent concentric layers were not observed. Therefore, the reasons for the existence of differential etching and the formation of concentric patterns in calcareous sponge spicules are still unclear.

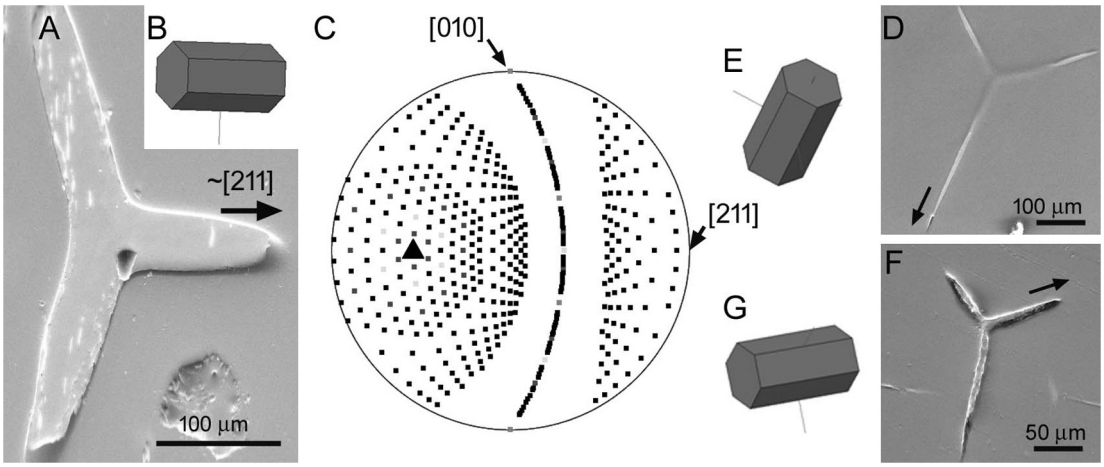

Fig. 5. Crystallographic analyses in the subclass Calcaronea. (A) SEM of a triactine spicule from *G. cylindrica*. The arrow indicates that the unpaired actine was elongated in the ~[2 1 1] direction. The hole near the centre of the spicule is an artefact caused during polishing. (B) 3D crystal model indicating the orientation of the spicule. The observation direction corresponds to the [8 4 −1] zone axis. (C) Stereographic projection representing the orientation of the spicule in (A) showing the principal directions of the calcite trigonal system. The *c*-axis is represented by a triangle. The [2 1 1] is the direction where the unpaired actine was elongated. (D) Triactine from *L. cirrhosa*. The unpaired actine was oriented in the ~[2 1 1] direction. (E) 3D crystal model of (D). (F) Pseudosagittal triactine spicule from *Heteropia* sp. The arrow indicates the unpaired actine and the ~[2 1 1] direction. (G) 3D crystal model of (F).

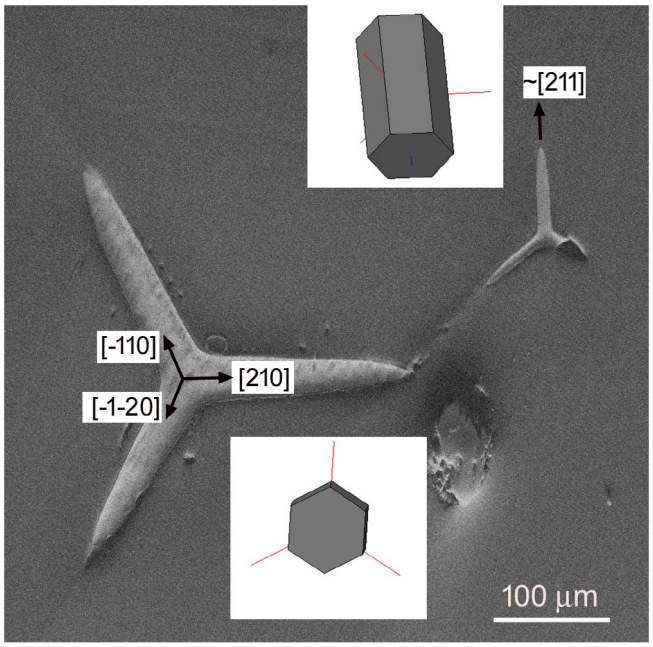

Fig. 6. Crystallographic orientations in the triactine spicules from *L. cirrhosa* (Calcaronea). The regular triactine (left side) was similar to the calcinean species (see the 3D crystal model at the bottom of the figure). The irregular triactine had the same orientation as the other Calcaronea species with the unpaired actine in the ~[2 1 1] direction (arrow). One paired actine from the irregular spicule was broken during the polishing (top right in the figure).

The successive concentric layers are likely formed by sclerocyte cell activities in a cyclical or discontinuous biomineralization process where the actines are grown layer by layer (Kopp et al., 2011; Sethmann and Wörheide, 2008). If this is the case, the sclerocytes would secrete one layer from the centre to the extremities followed by the successive layers covering the entire spicule. This proposition was not completely supported by *in vivo* assays using the fluorescent marker calcein, which showed a unidirectional growth from the centre to the extremities of the actines in triactine spicules from *Sycon* sp. (Ilan et al., 1996). However, in the case of the curved diactine from *Sycon* sp., Ilan et al. (1996) showed an alternative process in accordance with a cyclical growth process: (1) in the first moment, the fluorescent marker was observed at the tip of the spicule; (2) in the second moment, the extremity and a band near the centre were fluorescent; and (3) in the last step, 50% of the spicule was marked.

In the process of spicule formation, each pair of sclerocytes (founder and thickener cells) is responsible for the growth of one actine. From the concentric line pattern shown in the present study, we observed, in the triactine spicules, (see Fig. 1A and B) that the concentric layer of one actine is perfectly continuous with the layer from the adjacent actine. Considering a controlled cyclical growth process, each actine layer must grow synchronously with the other ones, and thus, the different sclerocytes should be coordinated during spicule formation to allow for continuity and symmetry of the layers. A strong biological control in the spicule biomineralization must occur to generate such a specific mineralized structure.

In the present work, different concentric layer patterns were observed, which may help to interpret the structure in 3D and, thus, the process of biomineralization of the spicules. In the species *L. serrata*, two lamination patterns were found in the same spicule type. Successive layers were observed concentrically surrounding (1) the centre of the spicule and (2) the centre of each actine. This variation was due to the difference in the plane in which the spicules were polished (thickness direction). To interpret this difference, a 3D model is presented (Fig. 8): the triactine spicule from *L. serrata* would be nucleated in a region corresponding approximately to the centre of the whole structure. Nucleation and growth of the actines would be controlled by the activity of the sclerocyte cells. The first deposited layers present a ellipsoidal pattern connected in the centre (Fig. 8A). Intermediates and more external layers have an approximately conical symmetry in each actine. Fig. 8B and C show sections of the spicule (parallel to the actines plane) more distant from the centre. Patterns of concentric layers surrounding each actine (Fig. 8B, section near the centre) and the entire spicule (Fig. 8C, section far from the centre) can be observed. When the triactine spicule is sectioned transversally to one actine, circular concentric lines are observed surrounding the central axis of the actine (Fig. 8D).

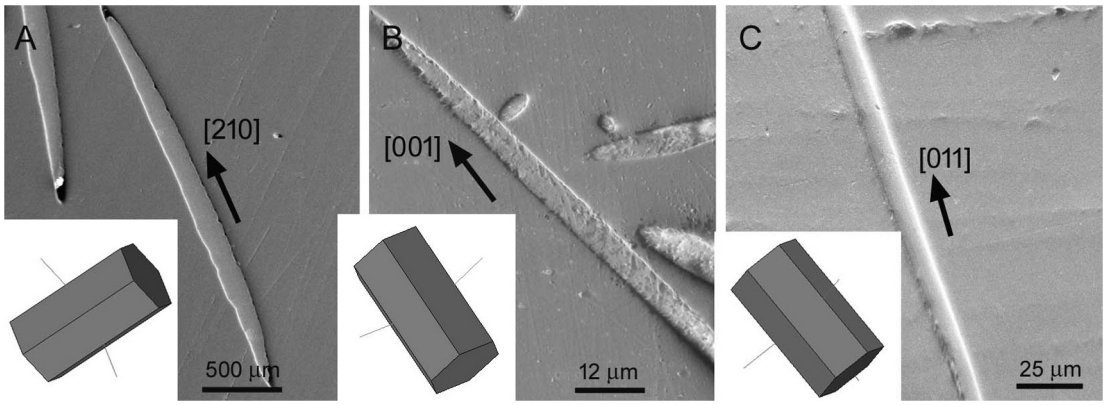

Fig. 7. Crystallographic analyses of the diactine spicules from the Calcaronea species. (A) Type I orientation: diactines oriented in the ~[2 1 0] direction (species with this orientation: *S. hastifera*, *Ute* sp., *Grantiopsis* sp. nov., *L. cirrhosa*, *Heteropia* sp. nov., and *G. cylindrica*). Image from *Heteropia* sp. nov. (B) Type II orientation: diactines oriented approximately in the [0 0 1] direction (species with this orientation: *Sycon* sp. and *T. labyrinthica*). Image from *Sycon* sp. (C) Type III orientation: diactines oriented in the [0 1 1] direction (only *Grantiopsis* sp. nov.). The inserts show crystal models representing the orientation of the calcite crystal in 3D.

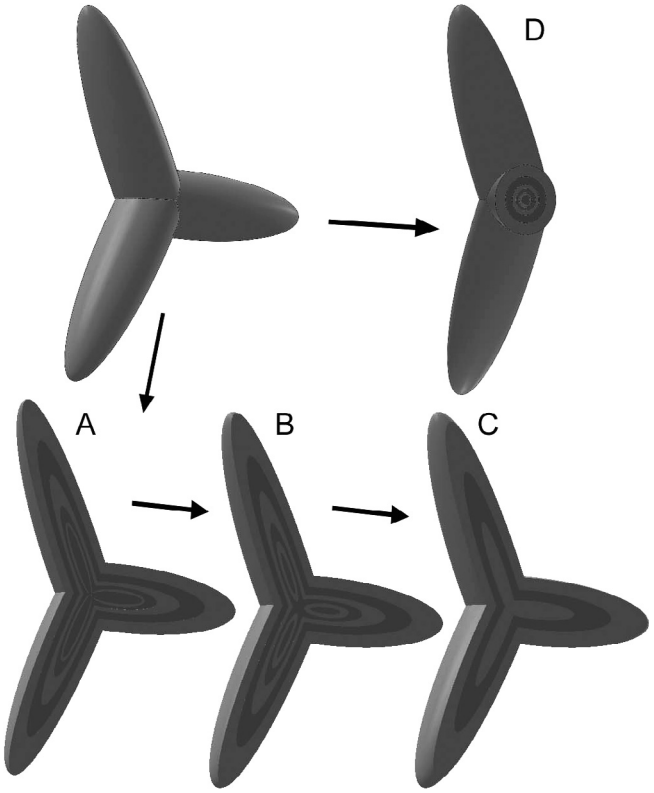

Fig. 8. A 3D model of the triactine spicule was created and sectioned at different depths to interpret the concentric layers observed by SEM. The spicule was formed by three ellipsoids connected at the centre. The additional external layers were conical. Figs. A-C show sections parallel to the plane of the actines (A) Section near the centre. (B) Intermediate section showing the concentric layers centred in each actine and the external concentric layers centred in the entire spicule (similar to Fig. 1A). (C) Section far from the centre showing only concentric layers surrounding the entire spicule (similar to Fig. 1B). (D) Transverse section of the actine showing the circular concentric layers.

4.2. Crystallographic orientation of spicules

The class Calcarea is subdivided into the subclasses Calcinea and Calcaronea, which have been proven to be natural groups due to their biological characteristics and through molecular phylogenetic analyses (Manuel et al., 2002; Voigt et al., 2012). Some of the morphological characters used by Bidder (1898) to define the subclasses were the orientation of the optical axis (equivalent to the *c*-axis in calcite) and the spicule morphology. In the subclass Calcinea the triactine spicules are regular and equiangular and "the optic axis of the spicules is nearly perpendicular to the walls of the sponge tubes." In the subclass Calcaronea, the triactine spicules are in general non-equiangular (mainly sagittal) and the "optic axes of the spicules vary in orientation according to the distance from the oscular rim". These definitions were proposed by Bidder (1898) following the works of Minchin (1896) and are still accepted currently (e.g., Klautau et al., 2013; Manuel et al., 2002; Rossi et al., 2011; Voigt et al., 2012). Whereas the crystallography and morphology of spicules from Calcinea are simple, only a few works have investigated in deep the crystallographic orientations in the subclass Calcaronea that presents irregular spicules.

The relation between the morphology of the spicule, its position in the body of the sponge and the orientation of the optical axis were previously investigated using polarizing light microscopy or crystallization overgrowth in the surface of the spicule (Bidder, 1898; Jones, 1954). Jones (1954) showed in the species *Leucosolenia complicata* (Calcaronea) that triactine spicules near the osculum (to a depth of 200 µm) had greater optic angle values (angle between the spicule plane containing the unpaired actine and the *c*-axis) than spicules closer to the base of the sponge. According to that work, the variation of the optic angle was between 20° and 34° whereas most spicules showed an optic angle close to 25°. The variation in the morphology of the spicule (dimension, shape and curvature of the paired actines) was not related to the variation in the optic angle. In the present work, the angle between the *c*-axis and the unpaired actine of the triactine spicules was between 27° and 37° (Fig. 9). Diactine spicules also showed variation in the crystallographic directions (Fig. 9).

The crystallographic direction of the triactine spicules from the 10 Calcaronea species (with one exception) described here was roughly the same (Fig. 5C), which was similar to *Sycon* sp. described previously by X-ray diffraction (Aizenberg et al., 1995) and to *P. magna* described by electron diffraction in FIB sections (Rossi et al., 2014). The unpaired actine was oriented between the ⟨2 1 1⟩ and ⟨632⟩ directions. The paired actines were elongated in symmetrically related directions showing that the symmetry in the form of the spicule is supported by the symmetry of the calcite crystal. The plane of symmetry that divides the paired actines was the {1 1 0} plane (plane perpendicular to ⟨0 1 0⟩ direction).

The data showed that spicules with different morphologies, dimensions and positions in the sponge body (e.g., pseudosagittal spicule, curved paired actines, small and giant spicules) had the

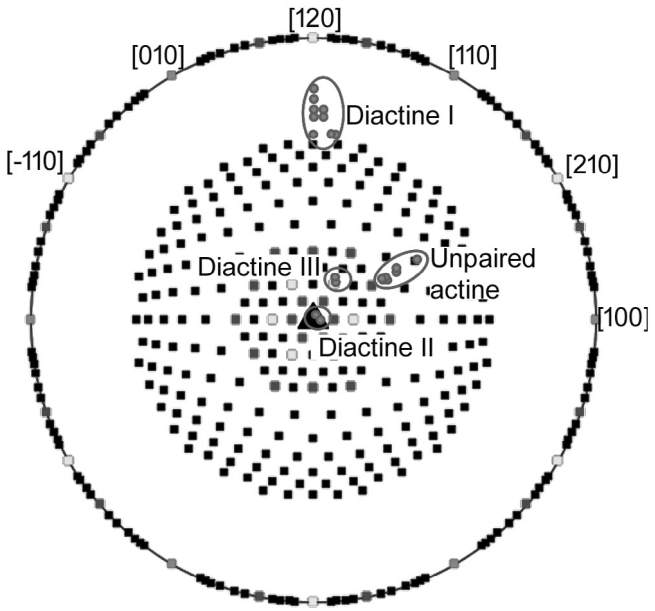

Fig. 9. Stereographic projection showing the crystallographic directions of the unpaired actines from the calcaroneans triactines and type I, II and III diactines. The triangle in the centre represents the *c*-axis. The dots show the variation in the orientation of the diactines and triactines found in different samples. For instance, the maximum angular variation in the orientation of the triactines was 10°.

same crystallographic orientation, which indicates a common evolutionary origin of the triactine spicules or a crystallographic restriction imposed by calcite. Only one spicule from a Calcaronea species had a different orientation. The species *L. cirrhosa* (Calcaronea) has regular triactines with the same orientation as the Calcinea spicules (actine elongated in the ⟨2 1 0⟩ directions). This finding will be further discussed viewing the position of these spicules within the sponge body.

The triactines from the Calcinea species (*Pericharax* sp. nov. and *P. carteri*) had actines elongated in the ⟨2 1 0⟩ direction (direction perpendicular to the {1 0 0} plane, equivalent to the a* axes). The Calcinea species *M. phanolepis* has untypical plate-like spicules (scales) with the *c*-axis approximately perpendicular to the plane of the scales. The diapason-like spicules are elongated in the ⟨2 1 0⟩ and are perpendicular to the *c*-axis. The subclass Calcinea is divided into two orders: Clathrinida and Murrayonida. The latter contains sponges with a hypercalcified skeleton, such as *M. phanolepis*. According to the results, the crystallographic orientation of the spicules from *M. phanolepis* is similar to that found in Calcinea, which supports its classification in this subclass but not necessarily in a separate order.

In the present work, the diactine spicules had three possible orientations: (I) the diactines are elongated in the [210] direction (*G. cylindrica*, *Grantiopsis* sp. nov., *Heteropia* sp. nov., *L. cirrhosa*, *S. hastifera*, and *Ute* sp.). This orientation was also reported before for the curved diactines from *Kebira uteoides* identified by X-ray (Aizenberg et al., 1995). Diactines with different sizes, morphologies and positions in the sponge body were grouped together with this orientation. For instance, the diactines from *Heteropia* sp. nov. and *Ute* sp. are tangentially orientated to the cortex, whereas the others are obliquely or perpendicularly oriented. *Heteropia* sp. nov., *L. cirrhosa*, and *Ute* sp. have fusiform diactines whereas the others with this orientation have arrow-shaped diactines or at least one tip different from the other. In the type (II) orientation, spicules are elongated in the [0 0 1] direction (*Sycon* sp. and *T. labyrinthica*). Slender diactines from *Sycon* sp. and *L. complicata* reported previously are also elongated in the *c*-axis (Aizenberg et al., 1995; Jones, 1954). In the type (III) orientation, the diactines were elongated in the [0 1 1] direction (*Grantiopsis* sp. nov.). Aizenberg et al. (1996) reported a diactine spicule from *Kebira* sp. elongated in the [2 1 1] direction. In that case, the triactine must have been ~~as~~ the ancestral spicule of the diactine because the unpaired actine of the Calcaronea triactines has the same elongation direction.

4.3. Spiculogenesis and skeletogenesis in calcareous sponges

The differences in the crystallographic orientations between Calcinea and Calcaronea; triactine and diactine; and the small angular variation in spicules from the same type are possibly related with mechanical forces caused by the environmental conditions.

In higher animals, both in soft and in mineralized tissues, complementary controls of cell and tissue structures and functions are additive to gene expression controls. Signals inform cells on mechanical pressures that are dependent upon the environmental conditions. Calcarea are frequently attached to rocks in the intertidal or shallow environments being exposed to waves and harsh water conditions. Alternatively, they can grow in deeper environments on sand or mud, and in this case, the basal spicules, which are frequently diactines or tetractines, grow in "anchors" with a very long major actine clearly in response to mechanical demands. In higher animals, bone tissues are strictly dependent upon mechanical pressure stimulation for both growth and mineralization.

The existence of these mechanical signalling pathways is poorly known in sponges, but the spicule form, which has been described in many Calcaronean and in some Calcinean sponges, is suggestive of their existence. The classical analysis performed by W.C. Jones (1954), which was mentioned previously, where the optic angle (the angle between the spicule plane containing the unpaired actine and the *c*-axis) increases closer to the oscular rim of *Leucosolenia* is an example. This thin tubular membrane is sustained by a single spicule layer. This layer is in tensile equilibrium in its lower part where the elastic forces in the membrane upwards and downwards are equivalents. At the end of the tube, the free oscular rim does not offer the upwards-down tension anymore; therefore, spicules progressively acquire a form similar to the letter "T" and maintain via their circular orientation, the smooth tube border. Many Calcaronea have an oscular rim, and all have the same modification observed in the last triactine or tetractine rows of spicules.

Conversely, large equiangular triactines described in the present study in the choanosome of the calcaronean sponge *L. cirrhosa* correspond to a similar modification of the tensergic signalling in the opposite sense. All the calcareous sponges have a basic operational unit: a single hollow asconoid tube lined internally by choanocytes. Spicules are embedded in an elastic matrix and, in general, only a few spicules are required to maintain the tube. The longer the tube, the more it is exposed to tensions caused by the surrounding seawater. The growth can only proceed through the formation of secondary radial tubes observed in *Sycon*, which become coalescent and gives the sponge a solid structure. The classical evolution along the line Ascon-Sycon-Leucon exists only among Calcaronea. The leuconoid calcaronean sponges retain the basal tubular circulation with the skeleton offering support and integration for the water circulatory system. Spicules have an appropriate size to sustain the tubular elements of the circulatory system. In rare cases, the choanoskeleton contains supplementary giant triactines that are scattered approximately parallel to the cortex. This is the case for *L. cirrhosa* (Calcaronea). These regular spicules (crystallographic directions similar to Calcinea) are neither associated with the aquiferous system tubes nor subjected to any tension or

spatial restriction because they are much larger than the aquiferous tubular structures of the choanosome. Without any additional tensile stimulus, they return to the basal triradiate equiangular system, which is determined by the symmetry of calcite crystal.

A similar conclusion can be found in rare parasagittal spicules in Calcinea. When a tubular peduncle is found at the base of the spherical cormus, longitudinal tension is generated by the movement of the seawater. Sagittal spicules can, however, be found, such as those observed in *Clathrina lacunosa* when the peduncle is long, the cormus is large, and the tensile forces become sufficiently strong to cause morphological modifications of the spicule.

The conclusion is that both Calcinea and Calcaronea follow the basal geometry of an equiangular triradiate spicule pattern, which is imposed by the crystalline properties of calcite. However, Calcaronea have essentially tubular organization, and the tension lines along the tubes impose the sagittal morphology and crystallographic modifications of the spicules.

Finally, we should not forget that sponges are subjected to a continuous water flow, which can be slow and diffuse in some cases but can achieve a greater force in others. Again, long and complex tubular aquiferous structures in Calcaronea will sustain a greater shear stress. It is notable that the apical actines of the tetractines, which are always perpendicular to the basal triactine system that is located within the tube wall, are frequently curved at their distal tip and always follow the water flow. Shear stress controls the pattern of organization and the branching of the vascular systems in higher animals. The blood pressure may be greater than the pressure of the seawater in the calcareous sponge aquiferous system, but low rheological forces and the shear stress are responsible for the initial formation of blood vessels in the embryo with a very low initial blood flow. Little is known about the shear stress controls of spiculogenesis in calcareous sponges.

5. Conclusion

The crystallographic orientations in the spicules of calcareous sponges is evolutionarily conserved, with some exceptions. The EBSD technique proved to be of great importance for determining these orientations by analyzing polished sections of spicules. From the examples mentioned in Section 4.3, it appears that the spicules morphology arose to adapt to the environmental conditions but was constrained by the trigonal symmetry of calcite which allowed limited possibilities for the relationship between spicule morphology and crystallographic orientations. Modifications in spicule morphology may be in part associated with genes and proteins and in part related to epigenetic stimuli imposed by the environment and the modification of the cormus size/organization during evolution. A systematic study on the crystallography of spicules can contribute to bring more insights for understanding the evolution of this biomineral and the possible contributions from local mechanical forces.

Acknowledgements

We thank LabNano/CBPF for the electron microscopy facility. Authors were funded by fellowships and research grants from the Brazilian National Research Council (CNPq), the Coordination for the Improvement of Higher Education Personnel – Brazil (CAPES) and the Rio de Janeiro State Research Foundation (Fundação Carlos Chagas Filho de Amparo à Pesquisa do Estado do Rio de Janeiro – Brazil (FAPERJ).

References

Aizenberg, J., Hanson, J., Ilan, M., Koetzle, T.F., Addadi, L., Weiner, S., 1995. Morphogenesis of calcitic sponge spicules: a role for specialized proteins interacting with growing crystals. FASEB J. 9, 262–268.
Aizenberg, J., Ilan, M., Weiner, S., Addadi, L., 1996. Intracrystalline macromolecules are involved in the morphogenesis of calcitic sponge spicules. Connect. Tissue Res. 34, 255–261.
Aizenberg, J., Weiner, S., Addadi, L., 2003. Coexistence of amorphous and crystalline calcium carbonate in skeletal tissues. Connect. Tissue Res. 44 (Suppl. 1), 20–25.
Bidder, G.P., 1898. The skeleton and classification of calcareous sponges. Proc. R. Soc. London 64, 61–76.
Boury-Esnault, N., Rützler, K., 1997. Thesaurus of sponge morphology. Smithson. Contrib. to Zool. 1–55. http://dx.doi.org/10.5479/si.00810282.596.
Gilis, M., Grauby, O., Willenz, P., Dubois, P., Legras, L., Heresanu, V., Baronnet, A., 2011. Multi-scale mineralogical characterization of the hypercalcified sponge *Petrobiona massiliana* (Calcarea, Calcaronea). J. Struct. Biol. 176, 315–329.
Hooper, J.N.A., Van Soest, R.W.M., 2002. Systema Porifera. A Guide to the Classification of Sponges.
Ilan, M., Aizenberg, J., Gilor, O., 1996. Dynamics and growth patterns of calcareous sponge spicules. Proc. R. Soc. London B Biol. Sci. 263, 133–139.
Jones, W.C., 1954. The orientation of the optic axis of spicules of *Leucosolenia complicata*. J. Cell Sci. s3-95, 33–48.
Jones, W.C., 1955. The sheath of spicules of *Leucosolenia complicata*. J. Cell Sci. s3-96, 411–421.
Jones, W.C., James, D.W.F., 1972. Examination of the large triacts of the calcareous sponge *Leuconia nivea* grant by scanning electron microscopy. Micron 3, 196–210.
Klautau, M., Azevedo, F., Cóndor-Luján, B., Rapp, H.T., Collins, A., Russo, C.A. de M., 2013. A molecular phylogeny for the order Clathrinida rekindles and refines Haeckel's taxonomic proposal for calcareous sponges. Integr. Comp. Biol. 53, 447–461.
Kopp, C., Meibom, A., Beyssac, O., Stolarski, J., Djediat, S., Szlachetko, J., Domart-Coulon, I., 2011. Calcareous sponge biomineralization: ultrastructural and compositional heterogeneity of spicules in *Leuconia johnstoni* Carter. J. Struct. Biol. 1871.
Ledger, P., Jones, W.C., 1977. Spicule formation in the calcareous sponge *Sycon ciliatum*. Cell Tissue Res. 181, 553–567.
Manuel, M., Borojevic, R., Boury-esnault, N., Vacelet, J., 2002. Class Calcarea Bowerbank, 1864. Sist. Porifera 1708.
Minchin, E.A., 1896. Suggestions for a natural classification of the Asconidae. Ann. Mag. Nat. Hist. 18, 349–362.
Minchin, E.A., 1908. Materials for a monograph of the ascons. II. The formation of spicules in the genus Leucosolenia, with some notes on the histology of the sponges. Q. J. Microsc. Sci. 52, 301–335.
Rossi, A.L., Campos, A.P.C., Barroso, M.M.S., Klautau, M., Archanjo, B.S., Borojevic, R., Farina, M., Werckmann, J., 2014. Long-range crystalline order in spicules from the calcareous sponge *Paraleucilla magna* (Porifera, Calcarea). Acta Biomater. 10, 3875–3884.
Rossi, A.L., de Moraes Russo, C.A., Solé-Cava, A.M., Rapp, H.T., Klautau, M., 2011. Phylogenetic signal in the evolution of body colour and spicule skeleton in calcareous sponges. Zool. J. Linn. Soc. 163, 1026–1034.
Sethmann, I., Hinrichs, R., Wörheide, G., Putnis, A., 2006. Nano-cluster composite structure of calcitic sponge spicules – a case study of basic characteristics of biominerals. J. Inorg. Biochem. 100, 88–96.
Sethmann, I., Wörheide, G., 2008. Structure and composition of calcareous sponge spicules: a review and comparison to structurally related biominerals. Micron 39, 209–228.
Sollas, W.J., Society, R.D., 1885. On the physical characters of calcareous and siliceous sponge-spicules and other structures. Sci. Proc. R. Dublin Soc.. R. Dublin Soc.
Uriz, M.-J., 2006. Mineral skeletogenesis in sponges. Can. J. Zool. 84, 322–356.
Voigt, O., Wülfing, E., Wörheide, G., 2012. Molecular phylogenetic evaluation of classification and scenarios of character evolution in calcareous sponges (Porifera, Class Calcarea). PLoS ONE 7, e33417.